Effect of Substituents on the Thermal Transitions and Degradation Behavior of Poly[bis(R-phenoxy)phosphazenes]

T. N. Bowmer*

Bell Communications Research, Inc., Red Bank, New Jersey 07701

R. C. Haddon and S. Chichester-Hicks

AT&T Bell Laboratories, 600 Mountain Avenue, Murray Hill, New Jersey 07974

M. A. Gomez, C. Marco, and J. G. Fatou

Instituto de Ciencia y Tecnologia de Polimeros, Juan de la Cierva 3, 28006 Madrid, Spain

Received September 25, 1990; Revised Manuscript Received April 30, 1991

ABSTRACT: The glass-to-rubber (T_g), melting (T_m), and crystal–liquid crystal ($T(1)$) phase transitions of poly[bis(4-R-phenoxy)phosphazenes] with R = $(CH_3)_2N$– and $(CH_3)_3C$– were studied by calorimetry, X-ray diffraction, and optical microscopy. The crystallinity of these polymers depended strongly on the annealing conditions and heating/cooling rates as well as the size and polarity of the substituent (R) groups. These data were combined with previous results, and the phase transitions, crystallinity, and thermal stability were compared for a series of five poly[bis(R-phenoxy)phosphazenes] where R = $-C_2H_5$, $-C(CH_3)_3$, $-OCH_3$, $-SCH_3$, or $-N(CH_3)_2$. Large bulky side groups or polar substituents increased T_g values and inhibited crystalline formation. Although no simple relationship was found between $T(1)$ and the substituent size or polarity, the transitions for our five polymers were consistent with Magill's empirical correlation between $(T_m - T_g)/(T_m - T(1))$ and $T(1)/T_m$ for semicrystalline polyphosphazenes. This correlation suggested that side-chain mobility and the temperature range of conformational disorder, $T_m - T(1)$, were governed by steric interactions between side groups. The thermal degradation mechanism of poly[bis(R-phenoxy)phosphazenes] was found to depend on the polarity of the "R" substituent.

Introduction

Polyphosphazenes (PPPZ) are a broad class of inorganic polymers with phosphorus and nitrogen alternating in the backbone $(-(X_2)P{=}N-)_n$. An important characteristic of these polymers is the ease with which the properties can be modified by the introduction of different substituent groups.[1-5] Semicrystalline polyphosphazenes can have three transitions: the glass transition temperature (T_g), the thermotropic transition from the crystal to mesophase state denoted as $T(1)$, and the mesophase to isotropic melt transition (T_m). PPPZs that are symmetrically substituted with aryloxy side chains (X) are usually semicrystalline polymers and generally display thermotropic behavior.[6-14]

A number of recent papers have discussed the morphological and structural changes involved in the crystal–liquid crystal transitions of some PPPZs, as well as the kinetics of the mesophase and crystal formation.[15-20] In previous work,[21-24] we have studied the phase transitions and kinetics of mesophase formation for a series of substituted poly[bis(R-phenoxy)phosphazenes]

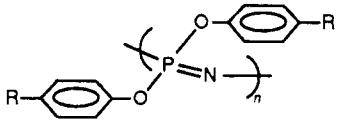

where R = $-OCH_3$, $-CH_2CH_3$, $-SCH_3$, or $-C(CH_3)_3$. All of them, except for poly[bis(*tert*-butylphenoxy)phosphazene] (PBTBPP), are semicrystalline polymers that form mesophases on melting of the crystallites. The PBTBPP case was particularly interesting since a liquid-crystal phase was formed from the liquid-crystalline glass with little or no crystallinity present.[22]

In this work, we extend our work on the thermal transitions of PPPZs to include the poly[bis(R-phenoxy)phosphazene] (PBDMAPP), where R = $-N(CH_3)_2$, which on doping has the highest reported conductivity found for a PPPZ.[25] In addition, the crystallization of PBTBPP will be described under various thermal and annealing treatments. Finally, we compare the thermal transitions and degradation behavior for five poly[bis(R-phenoxy)-phosphazenes] in terms of their chemical structure and reactivity of the R group.

Experimental Section

Synthesis. All the polymers were prepared by substitution reactions of the appropriate thallium aryloxide salts with poly(dichlorophosphazene). Elemental analysis of the polymers showed <0.2% residual chlorine. The ^{31}P NMR spectra were consistent with this high level of chlorine replacement. Gel permeation chromatography indicated an average molecular weight of 10^6 for all the polymers. The polymers were reprecipitated to remove any thallium salts. Small cyclic species (e.g., trimers, tetramers, etc., ...) should be removed during reprecipitation, and no evidence for cyclic species was found from ^{31}P NMR spectroscopy or chromatography analysis. Full details of the preparation technique were given elsewhere.[25]

Thermal Properties. Differential scanning calorimetry (DSC) was used to measure glass transitions, melting transitions, heats of fusion, crystallization exotherms, and decomposition exotherms. Typically, a 15–20-mg polymer sample was scanned at 10 °C/min between −50 and +250 °C with a Perkin-Elmer DSC-4/TADS system. A few scans were taken to 350–400 °C to observe exotherm transitions caused by main-chain scission or side-chain degradation. Although the heating rate was always 10 °C/min, cooling rates were changed as required to study crystallization kinetics.

Thermogravimetric analysis was performed on a Perkin-Elmer TGS-2/TADS system using ~5-mg samples that were heated at 10 °C/min from 50 to 800 °C. The purge gas was nitrogen from 50 to 600–700 °C when air was introduced into the carrier stream.

Morphological and Structural Analysis. Microscopy studies were carried out by using a Reichert transmitted polarized light microscope, fitted with a photomonitor to a Mettler FP80 central processor. The analog output was recorded on a strip

0024-9297/91/2224-4827$02.50/0

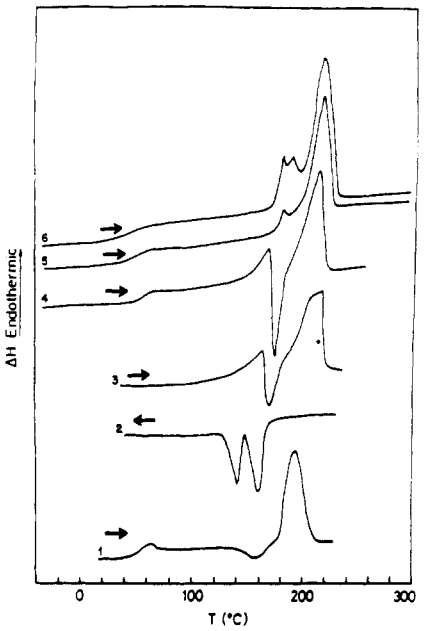

Figure 1. DSC curves for PBDMAPP with different thermal treatments (data from runs 1–5 are summarized in Table I).

chart recorder for thermooptical analysis (TOA). The melting and clearing temperatures were observed at various cooling and heating rates with a Mettler hot-stage FP82.

Wide-angle X-ray diffractograms were obtained from film samples held at a series of temperatures from room temperature to above $T(1)$. A Philips Geiger counter X-ray diffractometer and an Anton Paar high-temperature camera were used. The diffractograms were recorded in the 2θ range from 5° to 40° scanned at 2°/min using Ni-filtered Cu Kα radiation. Films were prepared by molding the polymers at temperatures above the $T(1)$ temperature and then crystallized under specified conditions.

Results and Discussion

The individual thermal behavior of PBDMAPP and PBTBPP will be described followed by a comparison of the thermal transitions and degradation behavior for the poly[bis(R-phenoxy)phosphazene] series.

(a) Poly[bis[4-(dimethylamino)phenoxy]phosphazene] (PBDMAPP). Figure 1 (run 1) shows the DSC scan for a PBDMAPP sample as prepared from solution. A glass transition, T_g, was observed at 60 °C while an exotherm centered at 150 °C was assigned to a crystallization process. An endothermic peak at 184 °C can be associated with the crystal–liquid crystal transition, as will be shown later by optical microscopy and X-ray diffraction data. The heat of fusion (ΔH_m) for the 184 °C transition was not large (21.4 J/g) compared with other polyphosphazenes,[2] which implied that either (1) the difference in order between the crystalline phase and the mesomorphic state was small or (2) the percent crystallinity was small.

The cooling process from 225 °C to room temperature at 10 °C/min (run 2 in Figure 1) showed two crystallization exotherms with peaks at 157 and 143 °C, which were designated as T_{cI} and T_{cII}, respectively. The following heat cycle at 10 °C/min (run 3) showed a melting endotherm with a peak at 166 °C, an exothermic crystallization peak at 170 °C, and a second melting endotherm at 200 °C. The 200 °C melting peak was broad, suggesting an envelope of multiple melting peaks. If the sample was cycled 3–4 times from −50 to +250 °C at 10 °C/min (heating and cooling), the same DSC profile was found with the T_m at 200 ± 1 °C and with a ΔH_m of 28 ± 0.5 J/g. Therefore, no

Table I
Thermal Data of PBDMAPP

run	remarks	T_g, °C	$\Delta C_p(T_g)$, J/g °C	$T(1)$,[a] °C	$\Delta H(T(1))$, J/g
1	original	60		184	21.4
2	crystallzn			157, 143*	23.9
3	melting	59	0.13	166, 200	28.0
4	melting	59	0.14	166, 201	20.1
5	melting	59	0.13	178, 203	32.2
6	melting	59	0.14	178, 185, 203	23.9

[a] Asterisk indicates maxima of crystallization peak. T_m = 260 °C (from TOA).

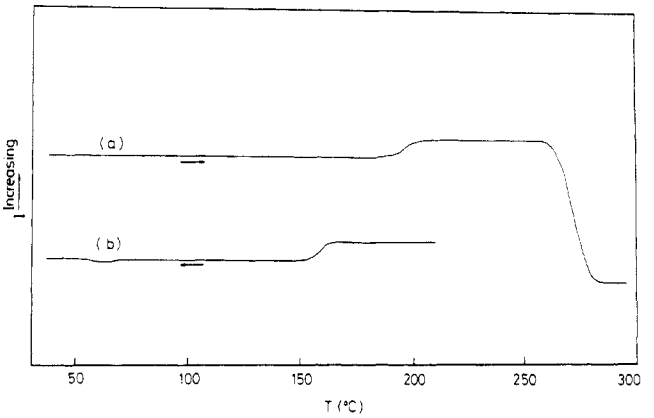

Figure 2. Thermooptical analysis of PBDMAPP: (a) heating, (b) cooling.

significant degradation occurred under DSC conditions, and the observed endothermic–exothermic transitions were assumed to reflect crystallite size and phase changes in PBDMAPP. The thermal stability of PBDMAPP will be discussed in more detail in section c.

It was assumed that the crystallites formed at T_{cII} melted at 166 °C, recrystallized at 170 °C, and finally melted again at ~200 °C along with the T_{cI} crystallites. A wide range of crystallite sizes would be expected for such a case and should result in a multiple melting transition, as was observed for the high-temperature transition (200 °C).

Table I lists the position and magnitude of the transitions as a function of the thermal history of the PBDMAPP sample. If a sample was quenched (>32 °C/min) from +250 to −50 °C, the subsequent heating scan (run 4) showed a melting endotherm with a maximum at 165 °C, followed by a crystallization exotherm with a maximum at 174 °C and a high-temperature melting transition at 196 °C.

However, very different DSC scans were obtained if PBDMAPP was isothermally crystallized before cooling to −50 °C. For example, runs 5 and 6 in Figure 1 were obtained from samples that had been crystallized at 160 °C for 1.2 and 18 h, respectively. The crystallization exotherm was absent, and multiple melting peaks were found between 170 and 210 °C. The sample annealed for the longer time at 160 °C showed even more melting transitions.

The highest melting peak (~200 °C) observed was assigned to the crystal–liquid crystal transition based on the TOA results shown in Figure 2a. The intensity increase at 200 °C corresponded to the crystal–liquid crystal transition. The birefringence increased at higher temperatures up to 260 °C, where a loss in light intensity was seen that was associated with the clearing temperature. This isotropic clearing transition was not observed by DSC, even in scans that approached the decomposition temperature of this polyphosphazene (i.e., 340 °C).

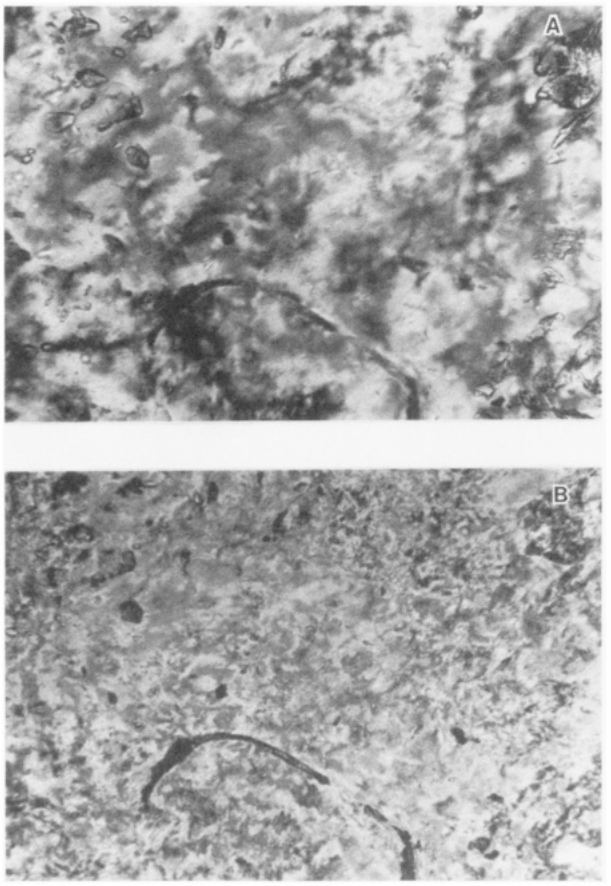

Figure 3. Optical microscopy photographs of PBDMAPP taken at (A) 200 °C and (B) 125 °C during cooling.

During cooling (Figure 2b), the decrease in intensity observed at 160 °C was correlated with the loss of the mesophase and the growth of crystallinity, as seen by optical microscopy (Figure 3). At 200 °C, PBDMAPP showed the typical birefringence of a liquid crystal (Figure 3A). If cooled to 125 °C, the birefringence disappeared and crystals were seen (Figure 3B).

The X-ray diffractograms in Figure 4 showed low levels of crystallinity in PBDMAPP between 25 and 190 °C. The reflections at $2\theta = 6.6, 7.0, 16.2$, and $20.2°$ were constant across this temperature range and in particular between 160 and 180 °C where multiple DSC peaks were found (Figure 1). On the basis of these X-ray results, crystal–crystal transitions or polymorphisms did not occur in PBDMAPP.

At temperatures above the crystal–liquid crystal transition, the reflections associated with crystalline order disappeared and only the mesophase reflection at $2\theta = 7.0°$ remained. The structure of the mesophase was assumed to be similar to that found in other polyphosphazenes[18,19,22] and described as a hexagonal packing of cylinders occupied by polymer chains with mobile backbones and side groups. Above the crystal–liquid crystal transition, the presence of the amorphous halo in the diffractogram (Figure 4) indicated that intermolecular order was preserved but the intramolecular order was lost.

(b) Poly[bis(4-*tert*-butylphenoxy)phosphazene] (PBTBPP). The DSC curve of PBTBPP, prepared from solution, is shown in Figure 5 (run 1). The glass transition temperature, T_g, was observed at 38 °C, and a series of endothermic peaks were found between 50 and 100 °C with a total heat of transition of 6.7 J/g. The multiple melting peaks were indicative of a broad distribution of crystallite sizes and degree of perfection. The isotropic

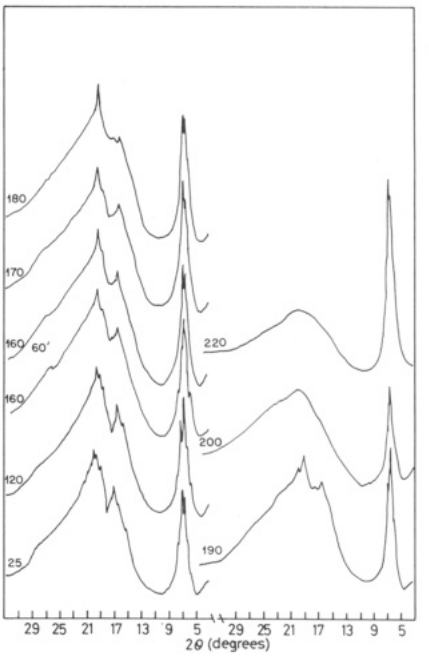

Figure 4. X-ray diffractograms of PBDMAPP at 25, 120, and 160 °C, 160 °C for 60 min, and 170, 180, 190, 200, and 220 °C.

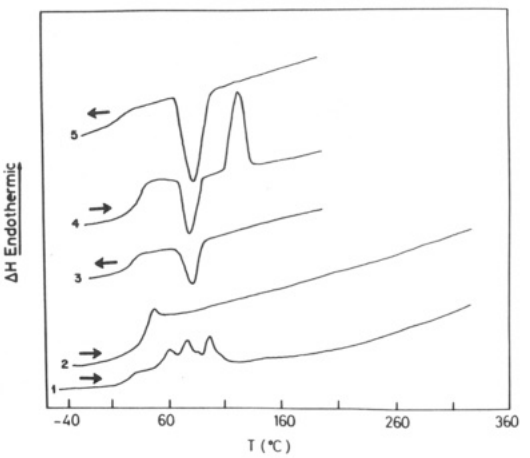

Figure 5. DSC curves for PBTBPP after thermal treatments listed in Table II.

transition was not observed by DSC up to 300 °C, a temperature above which the sample began to decompose (discussed in section d).

If PBTBPP was quenched from +200 to −50 °C, then the next heating curve (run 2) showed only a T_g at 51 °C with no endothermic peaks up to 300 °C. This peculiar behavior for a poly[bis(R-phenoxy)phosphazene] indicated that the 51 °C transition may not be a simple glass transition, as had been previously suggested.[22] We will show later from thermooptical and X-ray diffraction data that orientational order existed both below and above the 51 °C transition. The transition was interpreted as a change from a liquid-crystalline glass to a liquid crystal.

The DSC scans shown in Figure 5 and the transition data listed in Table II implied that, similar to other PPPZs, the thermal behavior of PBTBPP depended strongly on the sample's thermal history. The melting endotherms seen in run 1 (Figure 5) and the existence of conformational heterogeneities around 80 °C, found by ^{31}P NMR MAS/DD spectroscopy,[22] showed that small amounts of crystallinity can exist above T_g. The growth of these crystallites in PBTBPP was enhanced if the cooling rate from the mesomorphic state was reduced.

Table II
Thermal Data of PBTBPP

run	remarks	T_g, °C	$\Delta C_p(T_g)$, J/g °C	$T(1)$,[a] °C	$\Delta H(T(1))$, J/g
1	original	38	0.13	55, 80, 100	6.7
2	melting	51	0.15		
3	crystallzn	48		70*	3.3
4	melting	49		135	8.0
5	crystallzn			70*	10.9

[a] Asterisks indicate maxima of crystallization peak. Run 4 contained a crystallization peak at ~75 °C with ΔH_c of ~4 J/g.

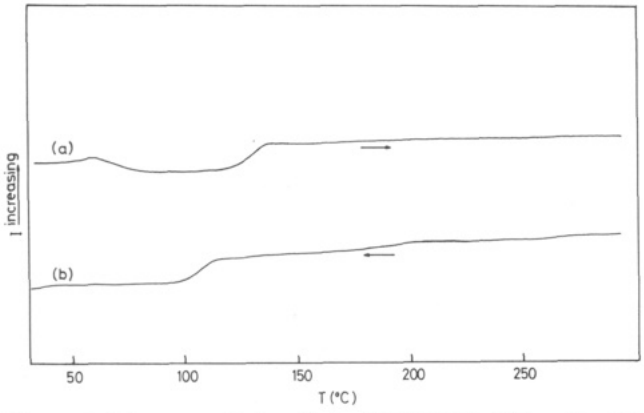

Figure 6. Thermooptical analysis of PBTBPP: (a) heating, (b) cooling.

If a sample was cooled at 10 °C/min from 200 °C (Figure 5, run 3), a small crystallization exotherm of 3.3 J/g was seen between 90 and 60 °C. In the subsequent heating cycle (run 4), a 4.1 J/g exotherm at 60–90 °C indicated that further crystallization from the amorphous fraction can occur. In addition, a crystal–liquid crystal transition was observed at 135 °C, with an enthalpy change of 7.9 J/g. If the sample was cooled slowly at 3 °C/min from 200 °C (run 5), then a large 10.9 J/g crystallization exotherm was found with a maximum at 70 °C.

Some PPPZs can degrade at temperatures below 200 °C to form cyclic oligomers that may crystallize.[2] For PBTBPP, such cyclic compounds are not responsible for the 135 °C transition since (a) no degradation exotherms were observed during the first heating scan to 200 °C, (b) PBTBPP samples heated repeatedly to 200 °C and quenched to −50 °C showed the same heating scan as run 2 with a single transition at 50 °C, and (c) reheating at 10 °C/min after run 5 produced a similar scan to run 4 with a T_g of 50 °C and a $T(1)$ transition at 135 °C with a $\Delta H(T(1))$ of 8.6 J/g.

The thermooptical analysis of PBTBPP was performed at a variety of heating–cooling rates. If a sample was cooled at 10 °C/min from 300 °C to room temperature, the subsequent heating cycle (Figure 6a) showed a birefringence loss at 55 °C and an intensity gain at 140 °C. The first transition was associated with the growth of the smallest crystallites, and the second transition (140 °C) was associated with crystal–liquid crystal transition. No clearing transition was found below 300 °C. If the sample was cooled down at 10 °C/min (Figure 5b), a birefringence loss was observed around 100 °C that was assumed to show the formation of crystalline order.

These TOA results were complemented with observation of the sample with polarized light microscopy. Parts A and B of Figure 7 show microphotographs obtained during run 5 at 30 and 160 °C, respectively, that indicate the existence of orientational order at temperatures both below and above the glass transition (51 °C). Since the birefringence is associated with the mesophase, therefore, the mesophase not only was present below T_g but also persisted and was even favored at temperatures up to 160 °C.

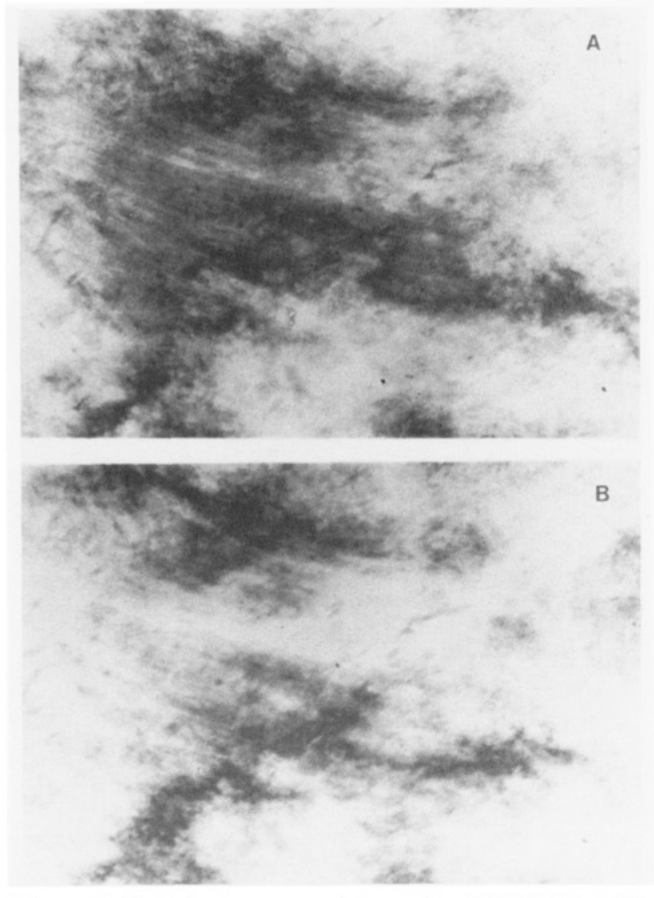

Figure 7. Optical microscopy photographs of PBTBPP at (A) 30 °C and (B) 160 °C during heating.

The analysis by X-ray diffraction at different temperatures confirmed the existence of the liquid-crystalline "glass". Figure 8 shows the diffractograms taken at 25, 80, 140, and 160 °C for a sample that was cooled from 160 °C to room temperature at 10 °C/min. At 25 °C, reflections associated with inter- and intramolecular order where found at 2θ = 6.4, 7.0, 8.2, 10.2, 16.0, and 17.4°. However, the intensity of these signals and the amorphous halo indicated that the percent crystallinity for the sample was low. Above T_g, the reflections remained constant in position but the intensity (i.e., percent crystallinity) increased by ~5–10% (Figure 8). The diffractogram was constant until 160 °C whereupon only the mesophase reflection at 2θ = 6.3° remained. The resonances from the three-dimensional crystalline order disappeared and were replaced by an amorphous halo centered at 16°.

In summary, the X-ray studies plus the DSC and TOA results showed, for the first time in PBTBPP, the existence of a mesophase below T_g and a crystal–liquid crystal transition. The apparent gain in crystallinity between T_g and temperatures approaching $T(1)$ implied that crystallization kinetics depended strongly on the annealing conditions. These effects were confirmed by WAXS analysis of a PBTBPP sample quenched from 160 °C to room temperature (Figure 9). Only the mesophase reflection at 2θ = 6.3° was found at room temperature with no indication of reflections from crystalline order. No crystallinity was detected if the sample was heated in 5 °C steps from 25 to 70 °C. However, at 100 °C the reflections caused by the three-dimensional crystalline structure were observed, and these reflections remained until the crystal–

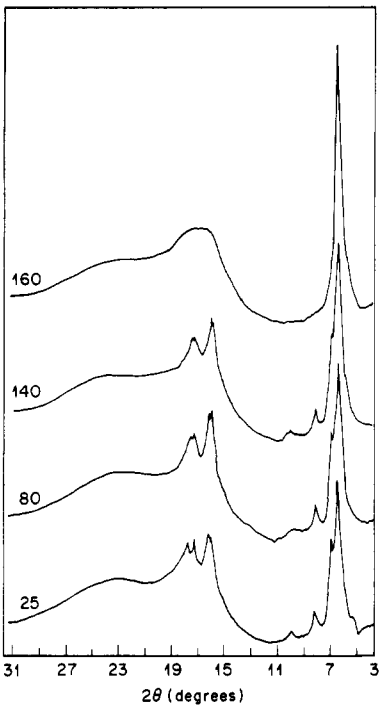

Figure 8. X-ray diffractograms of PBTBPP at different temperatures after slow cooling from 160 °C to room temperature.

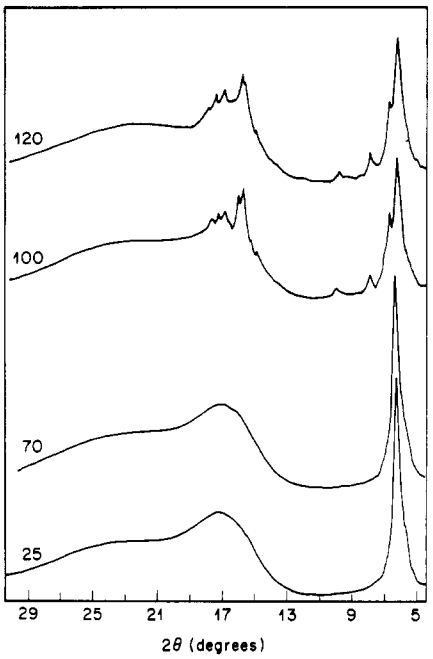

Figure 9. X-ray diffractograms of PBTBPP at different temperatures after the sample was quenched from 160 °C to room temperature.

liquid crystal transition ($T(1)$) was approached. These results showed that crystallinity was developed by annealing the existing mesophase, at temperatures between T_g and $T(1)$.

(c) Thermal Transitions. Table III lists the thermal properties for the poly[bis(R-phenoxy)phosphazenes] we have studied in this report and previous work.[22-25] Included in Table III are the literature values[8] for the first member of the series, poly(bisphenoxyphosphazene), PBPP. Since the DSC profiles for PPPZs were dependent on thermal history, the magnitude and position of the thermal transitions listed in Table III were determined from polymer samples with uniform thermal histories; i.e., the samples were cooled at 10 °C/min from above the

Table III
Thermal Data of Several Polyphosphazenes

polymer	R	T_g, °C	$T(1)$, °C	1 - λ, %
PBPP	-H	-4	159	93
PBEPP	$-C_2H_5$	-16	90–110	68
PBMOPP	$-OCH_3$	16	152	82
PBMTPP	$-SCH_3$	37	142	67
PBDMAPP	$-N(CH_3)_2$	59	203	18
PBTBPP	$-C(CH_3)_3$	51	140	10

Table IV
Thermogravimetric Parameters

	calorimetry results: high temp scan		TGA results: profile parameters		
substituent ("R")	exotherm, °C	loss, wt %	onset °C	temp, °C	loss, wt %
$-C_2H_5$	>350	3	375		
				400	10
				540	87
				800 (air)	91
$-C(CH_3)_3$	>350	2	400		
				540	87
				600 (air)	88
				850 (air)	96
$-OCH_3$	>350	2	400		
				540	87
				700	50
				800 (air)	100
$-SCH_3$	267[a]	5	335		
				300	5
				540	41
				600 (air)	45
				800 (air)	55
$-N(CH_3)_2$	>310	2	400		
				540	47
				850 (air)	75

[a] After the decomposition exotherm (45 J/g), PBMTPP had become a glassy material with a T_g of 42 °C and no T_m < 300 °C.

polymer's $T(1)$.

The variations in T_g values and percent crystallinity can be explained in terms of the size and polarity of the substituent group. For example:

(a) Compare the *tert*-butyl case (PBTBPP) with the ethyl case (PBEPP). Since the bulky *tert*-butyl group restricted segment and chain motion much more than a small ethyl group, the T_g for PBTBPP was much higher than that for PBEPP; i.e., +51 °C compared to -16 °C. In addition, the *tert*-butyl group apparently inhibited interchain ordering and crystallite formation in PBTBPP, such that crystallization occurred very slowly even under the most favored annealing conditions.

(b) Compare the T_gs for the polymers with methoxy, thio, and amino substituents. The value of T_g increased from 16 to 37 to 59 °C as the substituent's size increased from methoxy (CH_3O-), to thio (CH_3S) to amino ($(CH_3)_2N$-).

These results indicate that the T_g value was primarily determined by the size of the substituent group. Polar interactions played a secondary role as illustrated by the PBMOPP case with the polar $-OCH_3$ group. Although the methoxy substituent (PBMOPP) is a similar size to the ethyl substituent (PBEPP), the increase dipole–dipole interaction was assumed to result in the increase in T_g from -16 (ethyl) to +16 °C (methoxy). Therefore, both the size and chemical nature (i.e., polarity) of the substituent group determine the thermal properties of PPPZs.

Crystallinity can be calculated from $\Delta C_p(T_g)$ and $\Delta H(T(1))$ values as previously discussed.[8] Magill[26] showed that the larger the side groups, the less facile the overall crystallization process. This relationship was found for

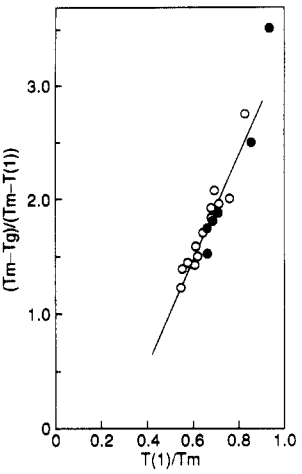

Figure 10. $(T_m - T_g)/(T_m - T(1))$ versus $T(1)/T_m$ for our polyphosphazenes (●) and Magill's[19] polymers (○).

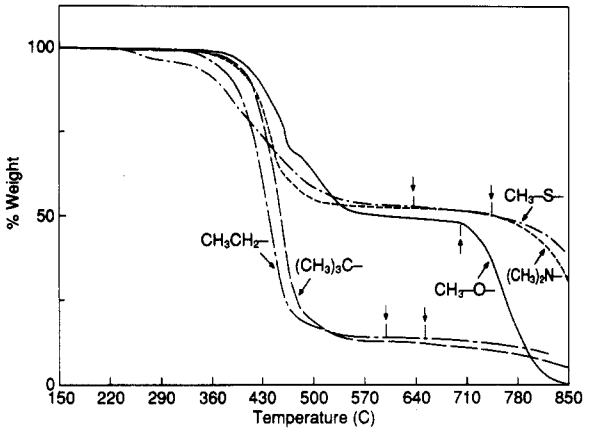

Figure 11. TGA profiles for poly[bis(R-phenoxy)phosphazenes] with the "R" group shown adjacent to the appropriate profile. The arrows identify the position when air was introduced into the carrier stream.

our series of polymers with >80% crystallinity for polymers with small substituents (e.g., PBMOPP) and negligible crystallization in PPPZs with bulky substituents (e.g., PBTBPP).

The value of $T(1)$ for our PPPZs depended on both the polarity and size of the substituent group. There was no simple relationship between $T(1)$ and side-group dimensions. The individual quantitative contributions from group size and polarity are not clear at present. Empirically, $(T_m - T_g)/(T_m - T(1))$ was found by Magill[19] to be proportional to $T(1)/T_m$ for semicrystalline PPPZs. He concluded that the side-chain mobility and the temperature range of conformational disorder, $T_m - T(1)$, was governed by steric considerations between side chains. Our series of poly[bis(R-phenoxy)phosphazenes] were consistent with this empirical relationship as shown in Figure 10, where our data is plotted along with Magill's data.[19]

(d) Thermal Stability. Exposed to moderate temperatures (<350 °C), PBEPP, PBMOPP, PBDMAPP, and PBTBPP showed broad DSC exotherms at 320–350 °C and 2–3 wt % losses in TGA. However, the major phase transitions (T_g, T_m) were not significantly changed after such heating. On the basis of the reported thermolysis[28,29] of poly(bisphenoxyphosphazene), we assumed that, below 300 °C, these four polymers underwent main-chain scission without extensive depolymerization to small fragments. The least stable of our polymers was PBMTPP, which in a high-temperature DSC scan produced a large exothermic peak ($\Delta H_{reaction}$ = 46 J/g) at 270 °C with a concomitant ~5% weight loss. After cooling from 290 °C, this PBMTPP sample was a hard glassy material with a single T_g at 42 °C and no melting transitions.

The TGA scans to 800+ °C for our polymers (Figure 11) showed two distinct behaviors dependent on the structure of the "R" substituent on the phenoxy side group. The polymers with the alkyl, nonpolar substituents {R = CH_3CH_2–, $(CH_3)_3C$–} lost 90 wt % at 400 °C, forming a char that was stable up to 800 °C. The polymers with polar, heteroatom-containing substituents {R = CH_3O–, CH_3S–, $(CH_3)_2N$–} lost only 50 wt % at 400 °C, forming a residue that was stable up to 700–800 °C in air.

PPPZs have been found to degrade by a variety of mechanisms such as main-chain scission and depolymerization to monomer or small cyclic oligomers, as well as side-chain cleavage–condensation reactions leading to a –P=N– based networks.[2,28-30] For example, poly(bisphenoxyphosphazene) (PBPP) was shown to undergo main-chain scission below 250 °C and depolymerization above 300–400 °C to chiefly cyclic trimers with other higher oligomers. In contrast, the thermolysis of poly(diaminophosphazenes), $[-NP(NHR)_2-]_n$, was reportedly characterized by a tendency to undergo side-chain condensation and cross-linking reactions that produced a –P=N– matrix cross-linked via –N(R)– type bridges. Above 800 °C, amines were eliminated to form a P=N network.

The only structural variable in our series of poly[bis(R-phenoxy)phosphazenes] was in the R group, and therefore the chemistry or stability of these R groups determined the particular thermal degradation mechanism for each polymer. Poly[bis(R-phenoxy)phosphazenes] with alkyl, nonpolar R groups are assumed to undergo main-chain scission below 350 °C and depolymerization to cyclic oligomers above 400 °C to form a –P=N– based network residue. This reaction sequence was reported[28,29] for the R = H and CH_3 polymers, and the TGA and DSC data for our polymers with R – CH_3CH_2– and $(CH_3)_3C$– were consistent with this thermolysis mechanism. However, if the R group was polar {R = CH_3O–, CH_3S–, $(CH_3)_2N$–}, then the thermolysis mechanism was similar to that observed for poly(aminophosphazenes),[28,30] $[-N=P(NHR)_2-]_n$; that is, side-chain condensation and cross-linking reactions that produced high char values (~50%) at 500–700 °C. Analysis of volatile products and high-temperature residues is needed before a general mechanism can be postulated with confidence and the subtle differences, such as the low-temperature (260–270 °C) degradation of poly[bis[(methylthio)phenoxy]phosphazene], can be understood.

Summary

We have extended our study of the thermal behavior of the poly[bis(R-phenoxy)phosphazenes] and described the crystallization of poly[bis[4-(dimethylamino)phenoxy]-phosphazene] for the first time. The position and magnitude of the thermal transitions as well as the crystallization kinetics for this series of polymers have been discussed in terms of the size and polarity of the substituents. Large bulky side groups or polar substituents were shown to increase T_g values and inhibit crystalline formation. The role of the mesophase was shown to be crucial to crystallite formation in some polyphosphazenes. The thermal stability of this series of polymers was explored by thermogravimetric studies and the degradation mechanism was shown to depend on the chemical structure of the side groups (R) attached to the P=N backbone.

References and Notes

(1) Allcock, H. R.; Kugel, R. L.; Valan, K. J. *Inorg. Chem.* **1966**, *5*, 1709.
(2) Allcock, H. R. *Phosphorus–Nitrogen Compounds*; Academic Press: New York, 1972.
(3) Allcock, H. R. *Chem. Eng. News.* **1985**, *63*, 22.
(4) *Inorganic and Organometallic Polymer*; Zeldin, M., Wynne, K. J., Allcock, H. R., Eds.; ACS Symposium Series 360; American Chemical Society: Washington, DC, 1988.
(5) Schneider, N. S.; Desper, C. R.; Beres, J. J. In *Liquid Crystalline Order in Polymers*; Blumstein, A., Ed.; Academic Press: New York, 1978; Chapter 9.
(6) Singer, R. E.; Schneider, N. S.; Hagnauer, G. L. *Polym. Eng. Sci.* **1975**, *15*, 34.
(7) Schneider, N. S.; Desper, C. R.; Singler, R. E. *J. Appl. Polym. Sci.* **1976**, *12*, 566.
(8) Sun, D. C.; Magill, J. H. *Polymer* **1987**, *28*, 1245.
(9) Allcock, H. R.; Connolly, M. S.; Sisko, J. I.; Al-Shali, S. *Macromolecules* **1988**, *21*, 323.
(10) Kojima, M.; Magill, J. H. *Makromol. Chem.* **1985**, *186*, 649.
(11) Godovsky, Y. K.; Papkov, V. S. *Adv. Polym. Sci.* **1989**, *88*, 129.
(12) Kojima, M.; Satake, H.; Masuko, T.; Magill, J. H. *J. Mater. Sci. Lett.* **1987**, *6*, 775.
(13) Meille, S. V.; Porzio, W.; Allegra, G.; Audisio, G.; Gleria, M. *Makromol. Chem. Rapid Commun.* **1986**, *7*, 217.
(14) Meille, S. V.; Porzio, W.; Bolognesi, A.; Gleria, M. *Makromol. Chem. Rapid Commun.* **1987**, *8*, 43.
(15) Kojima, M.; Masuko, T.; Magill, J. H. *Makromol. Chem. Rapid Commun.* **1988**, *9*, 565.
(16) Kojima, M.; Magill, J. H. *Polym. Commun.* **1988**, *29*, 166.
(17) Kojima, M.; Sun, D. C.; Magill, J. H. *Makromol. Chem.* **1989**, *190*, 1047.
(18) Kojima, M.; Magill, J. H. *Polymer* **1989**, *30*, 1856.
(19) Kojima, M.; Magill, J. H. *Polymer* **1989**, *30*, 579.
(20) Masuko, T.; Okuizumi, R.; Yonetake, K.; Magill, J. H. *Macromolecules* **1989**, *22*, 4636.
(21) Tanaka, H.; Gomez, M. A.; Tonelli, A. E.; Chichester-Hicks, S. V.; Haddon, R. C. *Macromolecules* **1988**, *21*, 2301.
(22) Tanaka, H.; Gomez, M. A.; Tonelli, A. E.; Chichester-Hicks, S. V.; Haddon, R. C. *Macromolecules* **1989**, *22*, 1031.
(23) Gomez, M. A.; Marco, C.; Fatou, J. G.; Chichester-Hicks, S. V.; Haddon, R. C. *Polym. Commun.* **1990**, *31*, 308.
(24) Gomez, M. A.; Marco, C.; Fatou, J. G.; Bowmer, T. N.; Chichester-Hicks, S. V.; Haddon, R. C. *Macromolecules* **1991**, *24*, 3276.
(25) Haddon, R. C.; Chichester-Hicks, S. V. *Macromolecules* **1989**, *22*, 1027.
(26) Magill, J. H. *Polym. Prepr. (Am. Chem. Soc., Div. Polym. Chem.)* **1989**, *30*, 297.
(27) Haddon, R. C.; Stein, S. M.; Chichester-Hicks, S. V.; Marshall, J. H.; Kaplan, M. L.; Hellman, M. Y.; Bowmer, T. N. *Mater. Res. Bull.* **1987**, *22*, 117.
(28) Allcock, H. R.; McDonnell, G. S.; Riding, G. H.; Manners, I. *Chem. Mater.* **1990**, *2*, 425.
(29) Allcock, H. R.; Moore, G. Y.; Cook, W. J. *Macromolecules* **1974**, *7*, 571.
(30) White, J. E.; Singler, R. E.; Leone, S. A. *J. Polym. Sci., Polym. Chem. Ed.* **1975**, *13*, 2531.